Cross sections of O^{q+} $(q = 1 - 4)$ electron loss in collisions with He, Ne and Ar*

Lu Yan-Xia(鲁彦霞)†, Lu Xing-Qiang(路兴强), Song Xiang(宋 想), and Zhang Bo-Li(张泊丽)

School of Nuclear Science and Technology, University of South China, Hengyang 421001, *China*

(Received 21 April 2010; revised manuscript received 21 July 2010)

Electron-loss cross sections of O^{q+} $(q = 1-4)$ colliding with He, Ne and Ar atoms are measured in the intermediate velocity regime. The ratios of the cross sections of two-electron loss to that of one-electron loss R_{21} are presented. It is shown that single-channel analysis is not sufficient to explain the results, but that projectile electron loss, electron capture by the projectile and target ionization must be considered together to interpret the experimental data. The screening and antiscreening effects can account for the threshold velocity results, but cannot explain the dependence of the ratio R_{21} on velocity quantitatively. In general, the effective charge of the target atom increases with velocity increasing because the high-speed projectile ion can penetrate into the inner electronic shell of target atom. Ne and Ar atoms have similar effective charges in this velocity regime, but He atoms have smaller ones at the same velocities due to its smaller nuclear charge.

Keywords: ion–atom collision, cross section, electron loss

PACS: 34.50.Fa, 52.20.Hv **DOI:** 10.1088/1674-1056/20/3/033402

1. Introduction

Multiple-ionization of atoms by ions is one of the mose fundamental processes, the study of which is an important topic in atomic physics with important applications in plasma physics, fusion, upper atmosphere studies and many other technological areas. Due to this broad range of applications and also its role in the study of atomic collision dynamics, there have been many experimental results and theoretical papers, but few papers concerned with the multiple electron loss of projectiles have been presented.

This work is a sequel to previous studies[1−4] on electron ionization, excitation and capture in ion–atom collisions in a intermediate velocity regime between low velocities, where the molecular model is applicable,[5] and high velocities, where atomic perturbative models are useful.[6] The present work concerns projectile electron loss in the presence of other collision channels, which have a strong influence on the electron-loss cross sections.

In the simplest cases, the target atom can be treated as an effective charged particle. Therefore, single-channel analysis is sufficient to interpret the experimental results, such as the application of the plane-wave Born approximation (PWBA) to projectile one-electron loss.[7] In these cases, the loss process is basically due to the Coulomb interaction between the target nucleus and the active projectile electron. However, the role of the target electron cannot be ignored. Target electrons can play a dual role: they can screen the target nucleus, thereby decreasing the electron-loss cross section (screening process) and can also lead to electron–electron collision, thereby increasing the electron-loss cross section (antiscreening process).[8]

However, it has been previously shown that in the intermediate velocity regime, electron loss and capture may have to be considered simultaneously because they have the same order of cross sections.[8] The capture channel will decrease the individual electron loss cross section. In this paper the intermediate velocity regime is near the active-electron velocities of the target atom or projectile ion. Namely, the velocity for the outside electron is at the lower limit and the velocity for the related inner electron is at the upper limit. This requires a coupled-channel calculation, but this procedure is far from being straightforward at intermediate velocities. Simple approaches are useful in this context. Multichannel effects are taken into account through unitarity considerations within the independent-particle model framework.

For projectile electron loss, both screening and

*Project supported by the Special Foundation for Key Programs of Basic Research at its earlier stage, Ministry of Science and Technology, China(Grant No. 2002CCA00900) and by the Foundation for the Doctors of University of South China (Grant No. 5-2007-XQD-001).

†Corresponding author. E-mail: luyanxia_67@126.com

© 2011 Chinese Physical Society and IOP Publishing Ltd

antiscreening are effective.[8−10] For light targets, there have been successful models, such as the plane-wave Born approximation (PWBA).[9,11] For heavy targets, however, PWBA's calculated results conflicts with experimental data, such as those of Sant'Anna *et al.*[12] and Sigaud *et al.*[13] They found that the total cross section of projectile electron loss tends to saturation as the target atomic number increases. The same conclusion was presented by excited highly charged projectile ions colliding with neutral atoms.[14−18]

The first-order perturbative method has been unsuccessful in calculating the loss cross sections of screened projectile ions by heavy neutral screened target nucleus. The reason is that there are strong collisions at small collision parameters. This suggests that the projectile electrons are not perturbative.[19] On the contrary, the perturbative method can be applied to antiscreening effects because the effects exist between several electrons.[20] The coupled channel calculation can deal with the screening effects on total loss cross sections, as shown by Grande *et al.*[21] and McGuire *et al.*[22] This method made greater progress than the former, but only with partial success. This model cannot thoroughly explain the results with heavy target atoms. This paper aims to investigate the cross section ratios R_{21} of two-electron loss to one-electron loss on a projectile in the intermediate velocity region to deepen our understanding on the electron emission process in ion–atom collisions.

2. Experimental procedure

This work was done using the 2×1.7 MV tandem accelerator at Lanzhou University. The scattering-ion spectra were gained using the static-electric field deflection technique. The recoil-ion spectra were acquired using the time-of-flight technique. The double differential spectra were obtained using the coincidence technique.[1]

The signals were detected according to the processes

$$\mathrm{A}^{q+} + \mathrm{B} \rightarrow \mathrm{A}^{q'+} + \mathrm{B}^{i+} + (q' - q + i)e, \qquad (1)$$

where i is the number of electrons removed from the target atom and q' is the charge state of scattered projectile ion.

We obtained the absolute cross sections based on the following formula

$$\sigma^i_{qq'} = \frac{n^i_{q'}/\eta^i_r}{\Big[\sum\limits_{q'} (I^{q'}/\eta^{q'}_p)\Big] NLT}, \qquad (2)$$

where $n^i_{q'}$ is the number of coincident events; η^i_r is the detector efficiency for recoil ion B^{i+}; $I^{q'}$ is the number of scattered projectile ion $\mathrm{A}^{q'}$; $\eta^{q'}_p$ is the detector efficiency for scattered projectile ion $\mathrm{A}^{q'}$; N is the density of target atoms; L is the effective length of target gas; and T is the efficiency of the transport process for recoil ions. The detection efficiency for scattered projectile is nearly 100% in our experimental velocity region. The double differential cross sections were obtained for the processes O^{q+} $(q = 1-4)$ colliding with He, Ne and Ar atoms.

3. Experimental results and discussion

According to formula (2), we obtained the cross section ratios of two-electron loss to one-electron loss for projectile R_{21},

$$R_{21} = \frac{\sum\limits_i \sigma^i_{q+2}}{\sum\limits_i \sigma^i_{q+1}} = \frac{\sum\limits_i (n^i_{q+2}/\eta^i_r)}{\sum\limits_i (n^i_{q+1}/\eta^i_r)}. \qquad (3)$$

Figures 1–3 show the ratios R_{21} of oxygen ions colliding with He, Ne and Ar atoms, where the velocity unit is Bohr velocity.

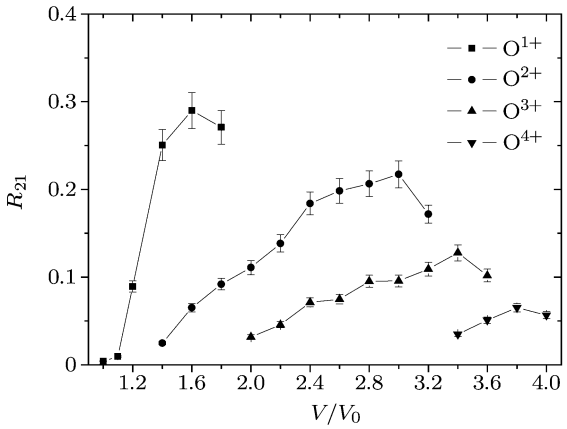


Fig. 1. Experimental ratios R_{21} for O^{q+} →He collisions $(q = 1-4)$.

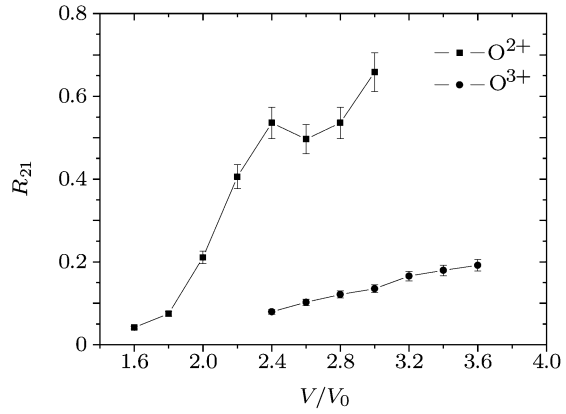


Fig. 2. Experimental ratios R_{21} for O^{q+} →Ne collisions ($q = 2, 3$).

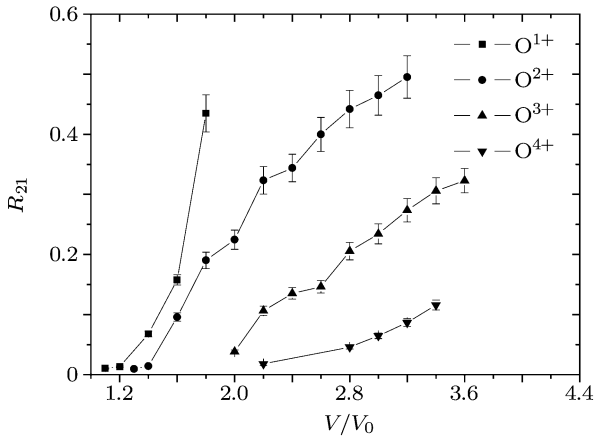


Fig. 3. Experimental ratios R_{21} for O^{q+} →Ar collisions ($q = 1 - 4$).

Figures 1–3 show that the ratios R_{21} depend intensively on velocity. We can draw the following results:

a) For differently charged ions colliding with the same target, the values of R_{21} are decreasing with the ion's charge state increasing at the same velocity. Furthermore, the higher the charge state, the higher the threshold of velocity at which the projectile losses two electrons. This suggests that the inner electrons on projectile ion are at the ground states during the whole collision process. The inner electrons at a lower energy level can not be excited to a higher energy level in our experimental velocity region.

b) The magnitudes of R_{21} for O^{2+} colliding with Ne and Ar atoms are similar. However, the magnitude of the curve for He atom is apparently lower. The screening and antiscreening theory can account for it. The Ne and Ar atoms have similar effective charges from smaller than one to several, but the He atom has the smaller effective charges from smaller than one to no more than two. As velocity increases, the collision will occur at a small collision parameter. The projectile ion can penetrate into the inner electronic shell of the target atom. Therefore, the effective charges for Ne and Ar atom will exceed that for He atom.

c) In the experimental velocity region, the maximum of R_{21} can be observed for the He target, but not for the Ne or Ar target. This indicates that the effective charge of He has reached the maximum value 2 at the velocity where the curves have the summits in Fig. 1. It can be inferred that the effective charges for Ne and Ar are still increasing as velocity increases. The maximum R_{21} for Ne and Ar will appear at some higher velocities. Exceeding the velocity, the magnitude of R_{21} will decrease down to a constant due to the shake-off mechanism.[6]

d) There is a dip in the O^{2+} colliding with Ne in Fig. 2, but no dip for He and Ar in Fig. 1 and Fig. 3, neither for other cases. We can expect the figure for O^{2+} colliding with Ne should present a saddle with an increase of the velocity since the maximum absolute cross sections of one-and two-electron loss for O^{2+} colliding with Ne appear at different velocities. The ratio R_{21} did present a saddle with velocity increasing as expected. In other cases, the velocity discrepancies for the two summits may be small. Thereby the saddle can not be observed unless the velocity step is very small. Due to few many-electron-loss cross section data, the multiple-ionization cross section of target atom can provide us with a reference to understand the figure in the intermediate velocity region.[23]

e) For a simple analysis, the ratios R_{21} can be deduced as $R_{21} \propto r_{q+2}^2/r_{q+1}^2 = E_{q+1}^2/E_{q+2}^2$, where E is the sequent ionization energy assuming the electrons on projectile ion are at the ground states. In general, the loss probability of the inner electron is smaller than that of outer electron. Thereby the maximum $R_{21}$are calculated as 0.41, 0.50, 0.46 and 0.68 for O^{+1}, O^{+2}, O^{+3} and O^{+4} ions, respectively. The experimental results are far from this analysis. The screening and antiscreening theory reminds us of the excited states of a projectile, especially for the outermost electron on projectile ion. Moreover, direct ionization (screening effect), Auger process, antiscreening effect and shake-off mechanism should be altogether taken into account for the electron loss of a projectile.

The threshold velocities were investigated for one- and two-electron loss of O^{+q} ($q = 1 - 4$). The results are shown in Table 1.

Table 1. Threshold velocities for electron loss of O^{+q} (Unit: Bohr velocity).

	O^{+1}_{loss1}	O^{+1}_{loss2}	O^{+2}_{loss1}	O^{+2}_{loss2}	O^{+3}_{loss1}	O^{+3}_{loss2}	O^{+4}_{loss1}	O^{+4}_{loss2}
He	0.8	1.1	1.1	1.6	1.6	2.4		3.6
Ne				1.6		2.4		
Ar	0.9	1.2	1.2	1.6	1.6	2.2	2.2	3.0

From Table 1, the threshold velocities for different targets are similar from the second to sixth columns. But for O^{+3}_{loss2} and O^{+4}_{loss2}, the threshold velocities for He target are obviously higher that those for Ar target. This can be explained by the screening effect. The high threshold velocities for the He atom are due to the low effective charge compared with Ar atom.

Table 1 shows that the threshold velocity for one-electron loss from $O^{+(q+1)}$ is the same as that for two-electron loss from O^{+q}. This indicates that the probability of losing the first electron from O^{+q} is nearly 100% at the threshold velocity.

4. Conclusion

This paper presents the experimental results of the ratios of one-electron loss R_{21} to two electron loss cross sections in the processes of O^{+q} colliding with He, Ne and Ar atoms in the intermediate-velocity regime. In general, the magnitudes of the ratios R_{21} increase as velocity increases. The peaks of the curves for the He target can be observed. The threshold velocities of emitting electrons from higher charged projectiles are higher than that of emitting electrons from lower ones. For the same targets, the magnitude of the ratio R_{21} is low for the highly charged projectile ion. The effective charges of Ar and Ne atoms are obviously bigger than that of the He atom according to the screening effect. Coupled-channel calculations are required to interpret the experimental results of total ionization cross sections, capture cross sections and electron loss cross sections in this velocity region. Recently, many domestic researchers have begun to investigate the cross sections of electron–atom collision,[24,25] excitation cross sections[26] and transfer cross sections.[27,28] All these studies can provide us with a deeper understanding on ion–atom collision processes.

Acknowledgements

This experiment was successfully done with the great assistance of Dr. Yu Deyang, Prof. Liu Zhaoyuan and Engineers Chen Zichun and Li Lanting. We thank them very much for their remarkable work.

References

[1] Lu Y X, Chen X M, Ding B W, Fu H B, Cui Y, Shao J X, Zhang H Q and Gao Z M 2007 *Acta Phys. Sin.* **56** 4461 (in Chinese)

[2] Chen X M, Lu Y X, Ding B W, Liu Y W, Cui Y, Gao Z M, Fu H B, Du J and Shao J X 2007 *Chin. Phys.* **16** 2384

[3] Chen X M, Lu Y X, Gao Z M, Cui Y, Liu Y W and Du J 2007 *Nucl. Instr. and Meth.* B **262** 161

[4] Lu Y X, Xiao D T, Yu T, Liu L J, Chen X M, Cui Y and Shao J X 2009 *Nucl. Instr. and Meth.* B **267** 474

[5] Sattin F 2001 *Phys. Rev.* A **64** 034704

[6] Matveev V I, Ryabchenko S V, Matrasulov D U, Rakhimov K Y, Fritzsche S and Stöhlker T 2009 *Phys. Rev.* A **79** 042710

[7] Wolff W, Luna H, Santos A C F, Montenegro E C and Sigaud G M 2009 *Phys. Rev.* A **80** 032703

[8] Montenegro E C, Sigaud G M and Meyerhof W E 1992 *Phys. Rev.* A **45** 1575

[9] Montenegro E C, Meyerhof W E and McGuire J H 1994 *Adv. At. Mol. Opt. Phys.* **34** 249

[10] McGuire J H, Stolterfoht N and Simony P R 1981 *Phys. Rev.* A **24** 97

[11] Senger B, Wittendorp R E and Rechenmann R V 1982 *Nucl. Instr. and Meth.* B **194** 437

[12] Sant'Anna M M, Melo W S, Santos A C F, Sigaud G M and Montenegro E C 1995 *Nucl. Instr. and Meth.* B **99** 46

[13] Sigaud G M, Jora's F S, Santos A C F, Montenegro E C, Sant'Anna M M and Melo W S 1997 *Nucl. Instr. and Meth.* B **132** 312

[14] Brendle' B, Gayet R, Rozet J P and Wohrer K 1985 *Phys. Rev. Lett.* **54** 2007

[15] Wohrer K, Chetioui A, Rozet J P, Jolly A, Fernandez F, Stephan C, Brendle' B and Gayet R 1986 *J. Phys.* B **19** 1997

[16] Xu X Y, Montenegro E C, Anholt R, Danzmann K, Meyerhof W E, Schlachter A S, Rude B S and McDonald R J 1988 *Phys. Rev.* A **38** 1848

[17] Chung H K, Lee R W and Chen M H 2007 *High Energy Density Physics* **3** 342

[18] Chabot M, Wohrer K, Chetioui A, Rozet J P, Touati A, Vernhet D, Politis M F, Stephan C, Grandin J P, Macias A, Martin F, Riera A, Sanz J L and Gayet R 1994 *J. Phys.* B **27** 111

[19] Walters H R J 1975 *J. Phys.* B **8** 54

[20] Woitke O, Za'vodszky P A, Ferguson S M, Houck J H and Tanis J A 1998 *Phys. Rev.* A **57** 2692

[21] Grande P L, Schiwietz G, Sigaud G M and Montenegro E C 1996 *Phys. Rev.* A **54** 2983

[22] McGuire J H 1987 *Phys. Rev.* A 36 1114

[23] Santos A C F, Melo W S, Sant'Anna M M, Sigaud G M and Montenegro E C 2001 *Phys. Rev.* A **63** 062717

[24] Liu J B, Wang Y and Zhou Y J 2007 *Chin. Phys.* **16** 0072

[25] Shi D H, Sun J F, Zhu Z L, Ma H, Liu Y F and Yang X D 2007 *Chin. Phys.* **16** 1655

[26] Yu C R 2008 *Chin. Phys.* B **17** 2097

[27] Chi B Q, Liu L and Wang J G 2008 *Chin. Phys.* B **17** 2890

[28] Zhu X L Ma X W Li B Feng W T Zhang S F Liu H P Qian D B and Zhang D C 2010 *Acta Phys. Sin* **59** 0620 (in Chinese)